ISSN 0023-1584, Kinetics and Catalysis, 2009, Vol. 50, No. 5, pp. 684–690. © Pleiades Publishing, Ltd., 2009.

Variations of Structure and Active Species in Mesoporous Cr-MSU-x Catalyst during the Dehydrogenation of Ethane with CO_2[1]

L.-Ch. Liu[a], H.-Q. Li[b], and Y. Zhang[b]

[a] *Department of Chemistry and Chemical Engineering, College of Environmental and Energy Engineering, Beijing University of Technology, Beijing 100022, China*

[b] *Institute of Process Engineering, Chinese Academy of Sciences, P.O. Box 353, Beijing 100080, China*

e-mail: lcliu@bjut.edu.cn

Received December 21, 2007

Abstract—The dehydrogenation of ethane to ethylene under CO_2 over mesoporous Cr-MSU catalyst was investigated with respect to the time on-stream behavior. When ethane was allowed to react for about 240 min, the meso-structure of catalyst remained nearly unchanged in spite of some decrease of surface area. The Cr(VI) species in tetrahedral coordination in fresh Cr-MSU were reduced to Cr(III) species in octahedral coordination, that was expected to cause the activity decrease of catalyst, together with the structure change. Cr(VI) is more active than Cr(III) for ethane dehydrogenation with CO_2, but Cr(III) represent fairly stable active centers for the reaction.

DOI: 10.1134/S0023158409050103

INTRODUCTION

The dehydrogenation of ethane to ethylene in the presence of CO_2 has been studied extensively [1–7]. The introduction of CO_2 could reduce the extent of deep oxidation which results in many by-products whereas ethylene selectivity drops when oxygen is used as oxidant. Moreover, by using greenhouse gas CO_2 as a soft oxidant it is possible to realize the recycle. From the results of many researchers, chromium oxide has been proved to be one of the most active catalysts for this reaction possibly due to its multi-valency [2–9].

MSU-x family, which structurally does not shows the long-range ordering, is an important silica-based mesoporous molecular sieve. Besides high surface area and adjustable uniform pore diameter, three dimensional wormlike channels of MSU are more favorable for the diffusion of molecular objects. Therefore, MSU is a promising catalyst support [10–12]. The incorporation of chromium into the MSU framework is expected to endow catalysts with high activity. In a previous study were reported the synthesis and catalytic performance of this Cr incorporated MSU (Cr-MSU) catalyst [13, 14]. The synthesized Cr-MSU catalyst exhibited higher activity and ethylene selectivity than many other catalysts in the dehydrogenation of ethane under CO_2. However, deactivation of Cr-MSU to a certain extent was observed simultaneously with reaction proceeding.

The activity of heterogeneous catalyst highly depends on the dispersion and oxidation state of active components as well as on the structural features of the support. Therefore, to investigate the structural transformation of Cr-MSU, and redox behavior of active Cr species in Cr-MSU catalyst during corresponding reaction is very important for elucidating the active sites, the reaction pathways and deactivation mechanism. Some researchers considered that coordinatively unsaturated Cr^{3+} ions are active sites for alkane dehydrogenation [15]. Such ions can attempt to restore the stable configuration of bulk Cr^{3+} ions by capturing molecules from gas phase. Mimura et al. [4] investigated the catalytic performance of Cr/HZSM-5 catalyst for oxidative dehydrogenation of ethane to ethylene with CO_2 as an oxidant. From TPR profiles of the Cr/HZSM-5 catalysts it can be inferred that, however, high oxidation states Cr species such as Cr(VI) is considered to be a key factor of higher activity.

The Cr-MSU prepared with Si/Cr molar ratio of 20, aging at 25°C for 22 h, with fatty alcohol polyoxyethylene ether as a template gave relatively high activities. In the present work, this Cr-MSU was selected as a typical catalyst to study its structure and oxidation state before and after reaction. Several techniques such as XRD, N_2-adsorption, XANES, DR UV-vis

[1] The article is published in the original.

and H_2-TPR were applied to characterize fresh and used catalysts. The dehydrogenation of ethane to ethylene over active chromium species is discussed based on characterization results.

EXPERIMENTAL

Catalyst Preparation

The Cr-MSU catalyst was synthesized according to our previous report [13]. Sodium silicate, chromium nitrate, fatty alcohol polyoxyethylene ether ($A(EO)_9$) were used as the source of silicone, metal and mesostructure-directing agent, respectively. The Si/Cr molar ratio was fixed to 20. The aging time and temperature were set to 22 h and 25°C. The actual chromium content was about 0.8 wt % (Inductively Coupled Plasma-Optical Emission Spectrometer, Perkin-Elmer).

Catalyst Characterization

The reaction of CO_2 and C_2H_6 over Cr-MSU was performed at atmospheric pressure in a fixed bed quartz reactor (5.0 mm i.d., 44.0 cm long) at 550–700°C. The reactants consisted were introduced with rates of 9 ml/min (CO_2) and 3 ml/min (C_2H_6). Catalyst loading was 0.2 g. Argon gas was introduced at a flow rate of 9 ml/min as balance gas when reaction was performed without CO_2. The products were analyzed on line by a gas chromatograph equipped with Porapack QS column (3 m, ∅1/4) and a thermal conductivity detector (Shimadzu GC 14B). The catalyst was collected and characterized when reaction was terminated after 240 min, it is designated as used Cr-MSU catalyst.

X-Ray diffraction (XRD) measurements were performed on X'pert Pro MPD X-ray diffractometer from PANalytical with CuK_α radiation ($\lambda = 0.154187$ nm), Generator Settings 40 kV, 30 mA, scanning speed at 0.017° and scanning regions at 0.5°–6.0°. N_2 adsorption/desorption isotherms were determined with Autosorb series ASIMP apparatus from Quantachrome. The samples were pretreated at 30°C under vacuum for 5 h before measurements. Calculation of the specific surface area (BET), pore volume and average pore size (BJH method) was made with the software of the apparatus.

X-Ray absorption spectroscopic measurements were conducted with synchrotron radiation at the National Synchrotron Radiation Laboratory (NSRL) (Heifei city, China). The synchrotron radiation facility is mainly composed of an 800 MeV electron storage ring with about 100–300 mA of ring current. The data were recorded in X-ray fluorescence mode at room temperature using a Si(111) double crystal monochromator. The energy step of measurement in the XANES region was 0.7 eV.

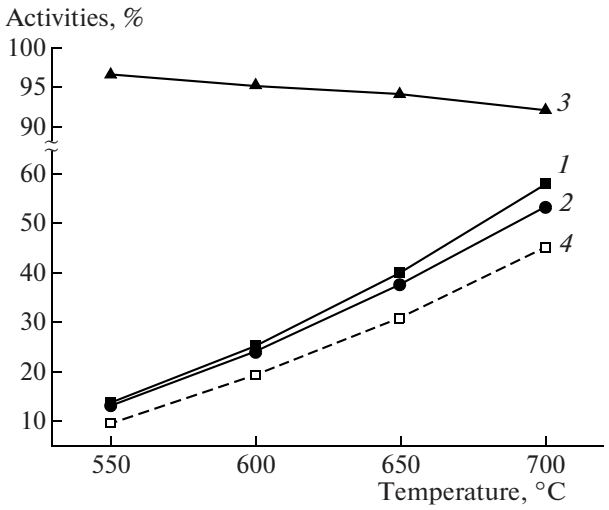

Fig. 1. Activity of Cr-MSU in the dehydrogenation of ethane to ethylene as a function of the reaction temperature. Ethane conversion (*1*), ethylene yield (*2*), ethylene selectivity (*3*) under CO_2; ethane conversion (*4*) under Ar.

Diffuse Reflectance UV-vis spectroscopic (DR UV-vis) measurements were recorded on a UV2100 spectrometer. The spectra were collected at 200–700 nm referenced to $BaSO_4$.

The H_2-TPR of the catalysts was performed on CHEMBET3000 chemical adsorption apparatus from Quantachrome by using a mixture of 5 vol % H_2/Ar as the reducing gas with a total flow rate of 20 ml/min. The 50 mg sample was heated from room temperature to 800°C at a heating rate of 16 K/min after being pretreated at 300°C for 60 min in He gas flow. The exit gas was cooled by mixture of *n*-octane and liquid nitrogen to condense the water generated from reduction of catalyst. The reduction signal was recorded by a TCD.

A Netzsch STA 499 TG/DTA instrument was used to obtain TG profiles. For clarity, the differential TG curve (DTG) was also presented. Approximate 20 mg of the sample was heated in air flow (100 ml/min) at a heating rate of 10 K/min.

RESULTS AND DISCUSSIONS

Catalytic Activities

The catalytic properties of Cr-MSU were investigated in the dehydrogenation of ethane to ethylene with CO_2. It is seen from Fig. 1 that the conversion of ethane increases while selectivity to ethylene decreases with the increase of the reaction temperature from 550 to 700°C. According to our measurements, the decrease in selectivity to ethylene is accompanied by increasing selectivity to methane which serves as the main by-product. The yield to eth-

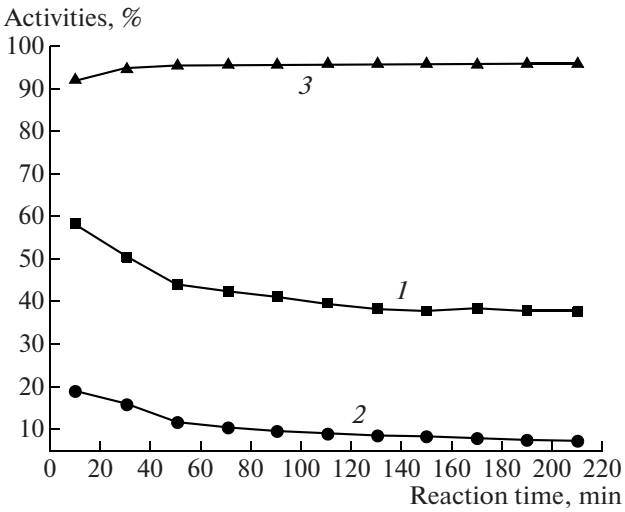

Fig. 2. Activity of Cr-MSU in dehydrogenation of ethane to ethylene under CO_2 as a function of the reaction time: *1*—conversion C_2H_6, *2*—conversion CO_2, *3*—selectivity C_2H_4.

ylene increases with temperature, which is consistent with the change of ethane conversion. Selectivity to ethylene is always above 90% at all investigated temperatures. When CO_2 in feed was substituted for argon, the conversion of ethane was reduced by 4–13% compared to the results under CO_2 at the same temperature. It suggested that CO_2 introduction enhanced ethane conversion to a certain extent. The catalytic performance over Cr-MSU with respect to time on stream is shown in Fig. 2. As reaction proceeds, the conversions of ethane and CO_2 decreases, indicating partial deactivation of catalyst. The conversion of ethane decreases from 58.0 to 37.6% in 3 h. The selectivity to ethylene gives little change.

Low-angle XRD Patterns and N_2 Adsorption

The low angle XRD patterns of fresh and used Cr-MSU catalyst are shown in Fig. 3. The fresh catalyst gives a clear diffraction peak at about $2\theta = 2°$ corresponding to d_{100} diffraction, suggesting the uniform meso-channels in catalyst [10, 17]. This characteristic peak still exists but becomes less intense for used catalyst. It is concluded that the meso-structure of Cr-MSU is preserved in spite of local destruction.

Figure 4 shows N_2 adsorption-desorption isotherms and pore size distribution curves for fresh and used Cr-MSU catalyst. There is little difference in pore size distribution between fresh and used catalysts. N_2 adsorption volume decreases for used catalyst. Based on XRD and N_2 adsorption results, some textural properties and structural parameters of fresh and used Cr-MSU were calculated and listed in table. As can be seen from the data the surface area decreases from 941 to 784 m^2/g, the average pore diameter remains almost unchanged while the pore volume decreases from 0.63 to 0.52 cm^3/g for the used Cr-MSU catalyst. The conclusion can be drawn that as the reaction proceeds local structure destroys and lattice shrinkage takes place for Cr-MSU-x resulting in the decline of surface area and pore volume of Cr-MSU. However, according to the results in Fig. 3 and table the major part of the mesoporous structure of used catalyst persists. The collapse of the meso-structure leads to the redistribution and loss of Cr species and consequently to the activity decrease. The conversions of ethane to ethylene and other by-products decrease simultaneously; therefore selectivity to ethylene shows little change for used Cr-MSU catalyst (Fig. 2).

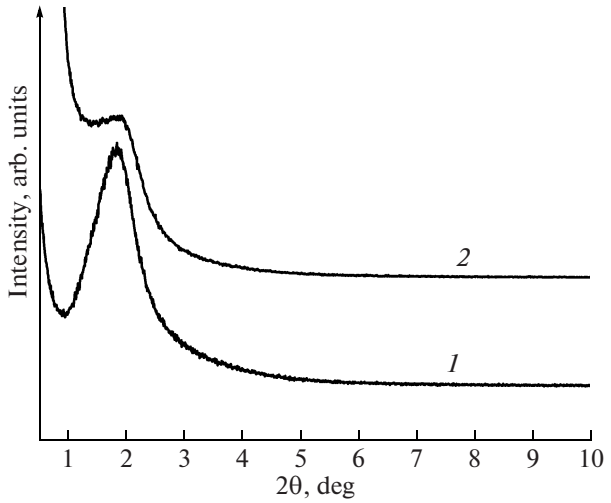

Fig. 3. Low angle XRD patterns of (*1*) fresh and (*2*) used Cr-MSU catalyst.

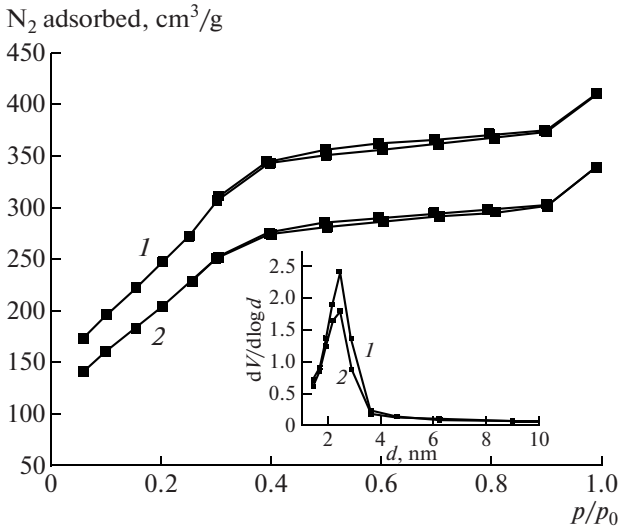

Fig. 4. N_2 adsorption-desorption isotherm and pore size distribution curve for fresh (*1*) and used (*2*) Cr-MSU catalyst.

Textural and structural parameters of fresh and used Cr-MSU

Sample	d_{100}, nm	Surface area, m^2/g	Pore diameter, nm	Pore volume, cm^3/g	Wall thickness, nm
Fresh	4.75	941	2.70	0.63	2.05
Used	4.50	784	2.68	0.52	1.82

Takehira et al. [16] showed the low-angle XRD patterns and structure properties of Cr-MCM-41 catalyst before and after the reaction between propane and CO_2.

However, they found that no significant changes occurring for both surface area and pore volume after reaction for 5 h with $N_2/CO_2/C_3H_8$ feed. They attributed it to the healing of lattice oxygen defect produced in reaction by oxygen from gas-phase CO_2. The structural differences between MCM-41 and MSU mesoporous molecular sieves may account for their different structure vibrations during similar reactions. Besides Takehira's work, there are few works devoted to the research of catalyst structure variation in a reaction, while more studies focused on the oxidation state of Cr species in Cr-based molecular sieves catalysts used for $CO_2 + C_2H_6$ reaction [5, 7]. This was also our research intention and would the corresponding results be presented below.

UV-vis, XANES, and H_2-TPR Studies

Diffused reflection UV-vis spectrums (DR UV-vis). The resulting UV-spectra of fresh and used catalysts are shown in Fig. 5. Two bands at $\lambda = 260$ and 370 nm in the charge transfer region are characteristic of the presence of Cr(VI) in tetrahedral coordination for fresh Cr-MSU catalyst. A weak shoulder at $\lambda = 450$–470 nm was ascribed to Cr(VI) in chromate ions [18]. The band at 370 nm becomes weaker for the used catalyst and two bands centered at about 450 and 620 nm corresponding to the $A_{2g} \rightarrow T_{1g}$ and $A_{2g} \rightarrow T_{2g}$ transitions of Cr(III) in octahedral symmetry appears [19, 20]. The results prove that the Cr species in fresh catalyst are Cr(VI) in tetrahedral coordination and they are reduced to Cr(III) after reaction. Zhao and Wang [7] found that the optical intensities of UV-bands of Cr-SBA-1 catalyst, in comparison with those of fresh catalyst, significantly decreased after dehydrogenation of ethane with CO_2 for 3 h. This is quite similar to our results, indicating the reduction of Cr species to lower oxidation state during the reaction.

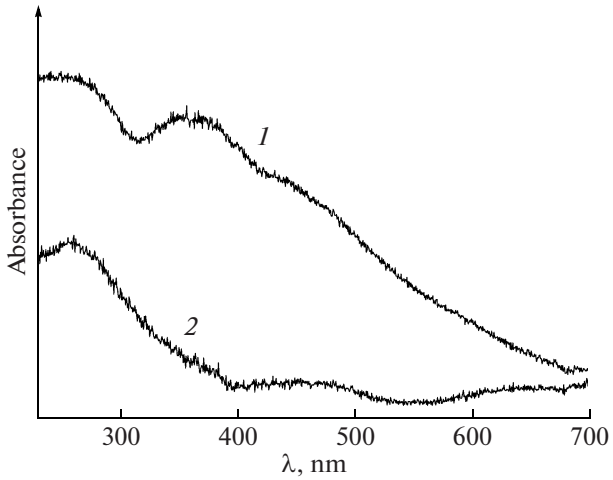

Fig. 5. DR UV-vis spectrums of fresh (*1*) and used (*2*) Cr-MSU catalyst.

Cr K-edge X-ray absorption near-edge structure (XANES). The Cr *K*-edge XANES spectra of standard $K_2Cr_2O_7$ and Cr_2O_3 are shown in Fig. 6 (curve *1* and *2*, respectively). A pre-edge peak at ca. 5994 eV in the spectra of $K_2Cr_2O_7$ is observed while no obvious pre-edge peak appears in the spectra of Cr_2O_3. It is well known that Cr(VI) atoms in CrO_4^{2-} or CrO_3 are present in tetrahedral coordination whereas those in Cr_2O_3 are

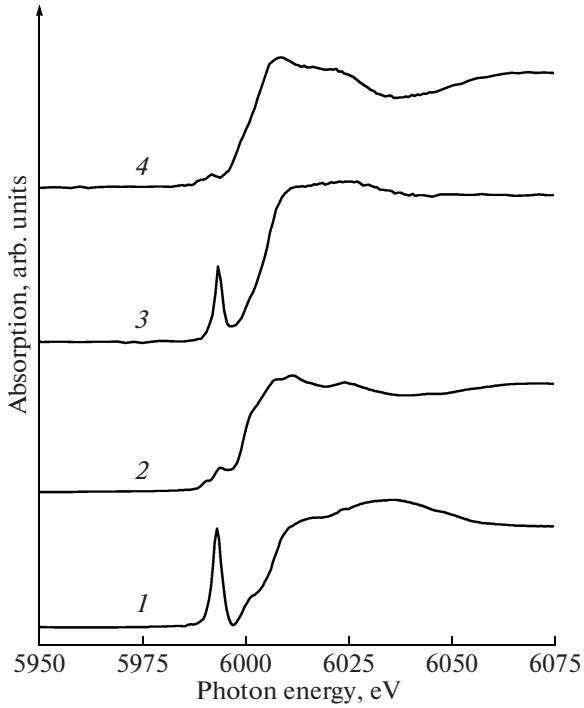

Fig. 6. Cr *K*-edge XANES patterns for $K_2Cr_2O_7$ (*1*); Cr_2O_3 (*2*); fresh (*3*) Cr-MSU and used (*4*) Cr-MSU catalyst.

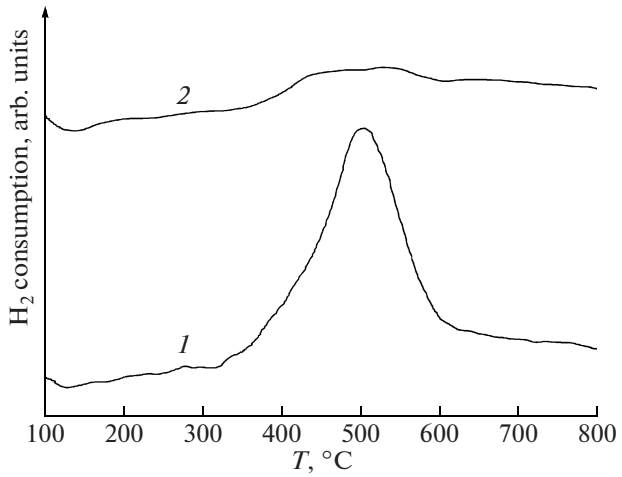

Fig. 7. H_2-TPR profiles for fresh (*1*) and used (*2*) Cr-MSU catalyst.

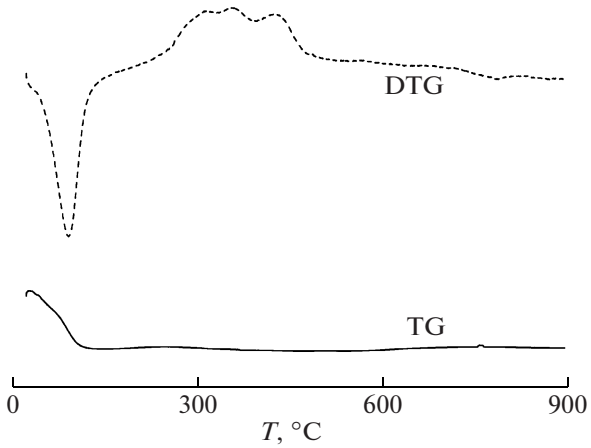

Fig. 8. Thermal gravity and differential thermal gravity curves of used Cr-MSU catalyst.

in octahedral environment. One to the presence of an antisymmetry center. The 1*s*–3*d* transition of Cr atoms is dipole forbidden for octahedral coordinated compounds such as Cr_2O_3. This dipole forbidden transition is permitted when the Cr-center is of non-central symmetry or 3*d* and 4*p* orbital are hybridized. So the intensity of pre-edge peak remarkably increases as the local symmetry around Cr-center changed from octahedral to tetrahedral coordination [16, 21]. As a result, a pre-edge peak can be observed in the Cr *K*-edge XANES spectra of CrO_4^{2-} (Na_2CrO_4, K_2CrO_4) and CrO_3 while no pre-edge peak appears in the spectra of Cr_2O_3. The Cr *K*-edge XANES spectra of fresh and used Cr-MSU-x are quite similar to those of $K_2Cr_2O_7$ and Cr_2O_3 respectively. The shape of the spectra changed from a Cr^{6+}- to a Cr^{3+}-type spectrum, including the disappearance of pre-edge peak, for used catalyst. It is suggested that Cr species in fresh Cr-MSU-x mostly are Cr(VI) in tetrahedral coordination, which are reduced to Cr(III) in octahedral coordination in the catalyst after reaction. The XANES analysis was also applied by Naoki Mimura [5] and Takehira [16] in their investigations. It was found that the Cr^{6+} (or Cr^{5+}) species in Cr/ZSM-5 was reduced to an octahedral Cr^{3+} species by treatment with ethane at 773 K [5]. Takehira's results on Cr-MCM-41 catalyst were very similar to ours that Cr(VI) in tetrahedral coordination was reduced to Cr(III) in octahedral coordination during propane dehydrogenation with CO_2 [16]. The XANES technique has been a strong tool to identify oxidation state and coordination of non-crystal species in catalyst.

H_2-Temperature programmed reduction (H_2-TPR). H_2-TPR technique was used to study the fresh and used catalysts and the obtained patterns are shown in Fig. 7. The fresh catalyst begins to be reduced from 350°C and shows one significant H_2 consumption peak at about 520°C, which is attributed to the reduction of Cr(VI) ⟶ Cr(III) [7, 8, 16]. This peak became weak and almost disappeared for the used catalyst, indicating most Cr(VI) species in catalyst have been reduced to Cr(III) after reaction and H_2 consumption peak corresponding to Cr(VI) ⟶ Cr(III) vanished. It is in accordance with above DR UV-vis and XANES results and previous results [5, 7].

Thermogravimetric analysis (TG). Carbon deposit on catalyst has always been considered to be one of important reason for catalyst deactivation during reactions of alkanes transformation. The TG and DTG curves of used Cr-MSU-x catalyst were measured and plotted in Fig. 8. There is no distinct weight loss signal except a water removal at about 100°C. Moreover, the used catalyst was studied by FT-IR and no adsorption signal of carbon contained species was observed. Therefore, the carbon deposit may not be significant in the present study and is ignored in the following discussion.

DISCUSSION

It is concluded from the above investigation that Cr species in Cr-MSU catalyst are Cr(VI) in tetrahedral coordination in the framework and on the inner/outer surface of the MSU support. Most Cr species are reduced to the Cr(III) in octahedral coordination after reaction. The activity decrease (deactivation) of the catalyst with reaction time was observed in Fig. 2. Therefore Cr(VI) species were the possible active sites for the reaction. It seemed that the reduction of Cr(VI) to Cr(III) caused the catalyst deactivation. Takehira and his coworkers summarized quite similar conclusion from their studies on Cr-MCM-41 catalyst [16]. Zhao and Wang gave the same expression that change in the valence state of chromium, namely tetrahedrally coordinated $Cr(VI)O_4$ existing on fresh Cr/SBA-1 catalysts was reduced to octahedrally coordinated Cr(III) to cause the deactivation of Cr/SBA-1

catalyst in ethane dehydrogenation with CO_2 [7]. However, we believe that this conclusion needs to be re-considered and modified taking in to account more reliable results. The Cr(III) species may be substituted for Cr(VI) species and act as the sites of lower activity because the catalyst still effects catalytic action despite partial reduction compared with the fresh sample. Based on these considerations, some possible reaction pathways are proposed.

The reaction pathways of ethane and CO_2 include reactions coupling and redox mechanisms [2–3, 6, 9]. The coupling reaction mechanism consists of direct dehydrogenation of ethane (I) and the reverse water-gas shift reaction (II). CO_2 could promote ethane dehydrogenation by consuming H_2 generated from ethane. This promoting effect is supported by the results of the enhancement ethane conversion in the presence of CO_2 described above. We believe that this process does occur in the reaction; however, the redox process is given more emphasis in the present discussion.

$$C_2H_6 \longrightarrow C_2H_4 + H_2, \quad \text{(I)}$$

$$CO_2 + H_2 \longrightarrow CO + H_2O, \quad \text{(II)}$$

$$3C_2H_6 + 2CrO_3 \longrightarrow 3C_2H_4 + Cr_2O_3 + 3H_2O, \quad \text{(III)}$$

$$3CO_2 + Cr_2O_3 \longrightarrow 3CO + 2CrO_3. \quad \text{(IV)}$$

Considering most Cr(VI) is in tetrahedral coordination in fresh Cr-MSU catalyst, the initial reaction process of ethane and CO_2 is believed to proceed according to equation (III) and (IV). Ethane is oxidized to ethylene by the Cr(VI) species of high oxidation state, which are simultaneously reduced to Cr species of lower oxidation state. The reduced Cr species are re-oxidized to Cr(VI) by CO_2 to complete a redox cycle and the dehydrogenation. However, Cr species of high oxidation state were irreversibly reduced to Cr species of low oxidation state in the reaction. Therefore, the reaction of ethane and CO_2 does not always obey equation (III) and (IV). This may result from a very weak oxidative ability of CO_2, which can not make the adequate regeneration of Cr(VI) by oxidation in time. Most Cr(VI) species were reduced to Cr(III) along the reaction. As indicated above, coordinatively unsaturated Cr^{3+} ions produced from reduction of Cr(VI) species on Cr-MSU catalyst became active sites. The dehydrogenation process can be described as follows. Initially ethane molecules adsorb on the active sites of coordinatively unsaturated Cr^{3+} ions, then C–H bond breaks off and –OH radicals and Cr–C band are formed. The ethylene molecules are produced and desorb from catalyst surface. Eventually, the –H ligands convert to H_2 or react with CO_2 to produce CO and water to accomplish the regeneration of the catalyst surface.

To sum up, Cr(VI) atoms in tetrahedral coordination form the main Cr species in fresh Cr-MSU-x catalyst and act as active sites in the dehydrogenation of ethane with CO_2 through redox mechanism. However, Cr(III) species turn out to be more stable active centers with reaction proceeding due to the irreversible reduction of Cr(VI) species. It follows adsorption-reaction-desorption sequence. Further experiments show that deactivated catalyst could be regenerated partially by treated with O_2 at 700°C. The re-oxidation of Cr(III) to Cr(VI) is also detected in the regeneration. These results indicate that the reduction of Cr species with high oxidation state is one of the reasons that accounts for the activity decrease of the catalyst.

CONCLUSIONS

The Cr-MSU-x catalyst exhibited good performance in dehydrogenation of ethane to ethylene with CO_2. Partial deactivation was detected in the reaction at the initial stage. The XRD and BET measurements suggest that the surface area and pore volume decreased during the reaction. The XANES-DR UV-vis and H_2-TPR methods suggested that most Cr species are Cr(VI) in tetrahedral coordination in fresh catalyst.

These Cr(VI) species were reduced after reaction. Both a structural deterioration and Cr species reduction lead to the initial decrease of catalyst activity. It is speculated that Cr(VI) species were active centers at the early reaction step. With the reduction of Cr(VI) species, Cr(III) species transform to generate more stable active centers for the reaction.

ACKNOWLEDGMENTS

The authors are grateful for the financial support of the National Science Foundation of China (granting no. 20436050), National Synchrotron Radiation Laboratory of China and Synchrotron Radiation fund of Innovation Project of Ministry of Education.

REFERENCES

1. Nakagawa, K., Okamura, M., Ikenaga, N., et al., *Chem. Commun.*, 1998, p. 1025.
2. Wang, S.B., Murata, K., Hayakawa, T., et al., *Appl. Catal., A*, 2000, vol. 196, p. 1.
3. Wang, S.B., Murata, K., Hayakawa, T., et al., *Catal. Lett.*, 2001, vol. 73, p. 107.
4. Mimura, N., Takahara, I., Inaba, M., et al., *Catal. Commun.*, 2002, vol. 3, p. 257.
5. Mimura, N., Okamoto, M., Yamashita, H., et al., *J. Phys. Chem. B*, 2006, vol. 110, p. 21764.
6. Deng, S., Li, H.Q., Li, S.G., et al., *J. Mol. Catal. A: Chem.*, 2007, vol. 268, p. 169.
7. Zhao, X.H. and Wang, X.L., *J. Mol. Catal. A: Chem.*, 2007, vol. 261, p. 225.
8. Zhao, X.H. and Wang, X.L., *Catal. Commun.*, 2006, vol. 7, p. 633.

9. Yang, H., Xu, L.Y., Ji, D.C., et al., *React. Kinet. Catal. Lett.*, 2002, vol. 76, p. 151.
10. Bagshaw, S.A., Prouzet, E., and Pinnavaia, T.J., *Science,* 1995, vol. 269, p. 1242.
11. Kim, S.S., Pauly, T.R., and Pinnavaia, T.J., *Chem. Commun.*, 2000, p. 835.
12. Kowalak, S., Stawinski, K., and Mackowiak, A., *Microporous Mesoporous Mater.*, 2001, vols. 44–45, p. 283.
13. Liu, L.C., Li, H.Q., and Zhang, Y., *J. Phys. Chem. B*, 2006, vol. 110, p. 15478.
14. Liu, L.C., Li, H.Q., and Zhang, Y., *Catal. Today*, 2006, vol. 115, p. 235.
15. Weckhuysen, B.M. and Schoonheydt, R.A., *Catal. Today*, 1999, vol. 51, p. 223.
16. Takehira, K., Ohishi, Y., Shishido, T., et al., *J. Catal.*, 2004, vol. 224, p. 404.
17. Sierra, L. and Guth, J.L., *Microporous Mesoporous Mater.*, 1999, vol. 27, p. 243.
18. Kustrowski, P., Chmielarz, L., Dziembaj, R., et al., *J. Phys. Chem. B*, 2005, vol. 109, p. 11552.
19. Rossi, S.D., Casaletto, M.P., Ferraris, G., et al., *Appl. Catal., A*, 1998, vol. 167, p. 257.
20. Gaspar, A.B., Brito, J.L.F., and Dieguez, L.C., *J. Mol. Catal. A: Chem.,* 2003, vol. 203, p. 251.
21. Requejo, F.G., Ramallo-López, J.M., Rosas-Salas, R., et al., *Catal. Today*, 2005, vols. 107–108, p. 750.